



Cite this: RSC Adv., 2016, 6, 28015

 Received 13th January 2016
 Accepted 3rd March 2016

 DOI: 10.1039/c6ra01087c
www.rsc.org/advances

Selective oxidation of organic sulfides to sulfoxides using sugar derived *cis*-dioxo molybdenum(vi) complexes: kinetic and mechanistic studies†

Noorullah Baig, Vimal Kumar Madduluri and Ajay K. Sah*

Six Mo(vi) complexes of 4,6-O-ethylidene- β -D-glucopyranosylamine derived ligands have been used for the selective oxidation of five organic sulfides to corresponding sulfoxides. The structure of a new sulfide $[(2\text{-}(2\text{-}(phenylthio)phenyl)imino)methyl]naphthalen-2-ol$ (S5) and its corresponding sulfoxide (S05) has been established using single crystal X-ray diffraction studies along with other routine analytical techniques. The yields of sulfoxides were calculated using HPLC and one of the catalysts was recycled five times without any appreciable loss in its activity. Kinetic studies on sulfoxide formation was performed on compound S5 using UV-visible spectroscopy, which suggested overall first order kinetics. A plausible mechanism for sulfide oxidation has been proposed based on our findings and previous literature reports.

1. Introduction

Sulfoxides are important from a biological as well as a chemical point of view due to their utility in drug development,¹ asymmetric synthesis² and oxo-transfer reagents like that in Swern oxidation.³ They are used in the preparation of several biologically and pharmaceutically important compounds like compactin, ML-236A (antihyperlipidimic agent),⁴ tacrolimus or FK-506 (immunosuppressive agent),⁵ 11-oxoquinolin methyl ether (steroid),⁶ and 12,13-epoxytrichothec-9-ene (having a wide range of biological properties)⁷ etc. In the context of organic synthesis, sulfoxides are used in carbon–carbon bond formation,^{8–10} the Diels–Alder reaction^{11–13} etc. Due to the versatile use of sulfoxides, their preparation from corresponding organic sulfides are well documented, however, the methods have several drawbacks like over-oxidation of the substrate to sulfone, longer reaction times, selectivity problems, and the use of strong oxidising agents like hydrogen peroxide (H_2O_2) and *meta*-chloroperoxybenzoic acid (*m*-CPBA)^{14–17} etc. Hence, the need of the current scenario is to develop an environmentally benign protocol having sustainable and greener reaction conditions. In this venture, we are developing the methodology for selective oxidation of organic sulfides into corresponding sulfoxides using glucose derived *cis*-dioxo Mo(vi) complexes as the catalyst. At the initial stage, we had optimized the

conditions for the oxidation of thioanisole (S1) to methyl phenyl sulfoxide (S01) with respect to the solvent, catalytic loading, reaction timing etc., and the findings have been already communicated.¹⁸ The best yield of sulfoxide was isolated from the reaction performed in ethanol, using commercially available urea–hydrogen peroxide (UHP) as a mild oxidant.

Molybdenum is one of the essential and less toxic metals, which easily form complexes with a variety of biologically important compounds like carbohydrates,^{18,19} porphyrins,^{20,21} flavins^{22,23} and amino acids.²⁴ It plays a vital role in the activities of xanthine oxidase, nitrate reductase, nitrogenase, DMSO reductase^{25,26} etc. Our initial success in the selective oxidation of S1 to S01 using the glucose derived *cis*-dioxo molybdenum(vi) complex under mild conditions, prompted us to make the methodology sustainable and reproducible for general organic sulfides. Along this line, we have used six complexes (Fig. 1), including two new ones as a catalyst for selective oxidation of organic sulfides to corresponding sulfoxides (Scheme 1). Five different sulfides were tested for oxidation, and the (%) formation of sulfoxides were obtained using the HPLC method. Turn over number and turn over frequency (per hour) were also calculated for all the reactions and the same were found in the range of 7.4–19.6 and 12–78 respectively.

Kinetic studies were performed on the oxidation of S5 using UV-visible spectroscopy and several control reactions were performed to ascertain the reaction paths of sulfide oxidation. Based on our current studies and the reported literature, we have proposed a plausible mechanism for this reaction. Hence, this paper deals with the synthesis of a new sulfide, selective catalytic oxidation of organic sulfides to sulfoxides using sugar derived *cis*-dioxo Mo(vi) complexes and mechanistic aspects of this oxidation reaction.

Department of Chemistry, Birla Institute of Technology and Science, Pilani Campus, Pilani, Rajasthan-333031, India. E-mail: asah@pilani.bits-pilani.ac.in; Fax: +91-1596-244183; Tel: +91-1596-515662

† Electronic supplementary information (ESI) available: Crystallographic data for structure S5 and S05. CCDC 1445051 and 1445052. For ESI and crystallographic data in CIF or other electronic format see DOI: [10.1039/c6ra01087c](https://doi.org/10.1039/c6ra01087c)

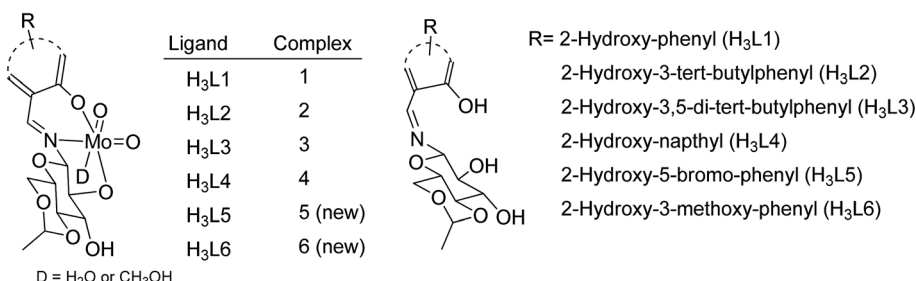


Fig. 1 *cis*-Dioxo molybdenum(VI) complexes of H₃Ln.

2. Experimental

2.1. General

5-Bromosalicylaldehyde, *ortho*-vanillin, 2-(phenylthio)aniline (S4), 2-hydroxy-1-naphthaldehyde and UHP were procured from Sigma-Aldrich India, while diphenyl sulfide (S2), benzyl phenyl sulfide (S3) and molybdenum(VI) oxide bis(2,4-pentanedionate) [MoO₂(acac)₂] were from Alfa Aesar. The complexes 5 and 6 were synthesized following the procedure reported for complex 1.²⁷ All other chemicals and solvents were purchased from local vendors and solvents were purified and dried following the standard methods before use. All the experiments were performed at room temperature under normal atmospheric conditions.

UV-visible absorption spectra were recorded on a Shimadzu UV-260 spectrophotometer and FTIR spectra on an ABB Bomen MB 3000 FTIR machine using a KBr Matrix. ¹H and ¹³C NMR spectra were recorded in DMSO-d₆ and CDCl₃ on a Bruker Avance spectrometer and data was processed using MestReNova software. HRMS and ESI-MS were recorded on a Thermo scientific Q EXACTIVE and Hewlett-Packard' HP GS/MS 5890/5972 mass spectrometer respectively. The yields of sulfoxides were calculated by HPLC separation using a Waters Sunfire C-18 column of 5 µm, 4.6 × 250 mm, a flow of 0.85 mL min⁻¹; wavelength of 315 nm; temperature of 28 °C; injection volume of 20 µL; eluent of water/MeOH (v/v) 0.18/0.67. Calibration was done using 30, 40, 50, 60, 70 and 80 ppm, of sulfoxide solutions.

Single crystal X-ray diffraction data were collected on a Rigaku XtaLAB mini diffractometer using graphite monochromated Mo-K α radiation. An empirical absorption correction was applied on the data and all calculations were performed using the CrystalStructure²⁸ crystallographic software package except for refinement, which was performed using

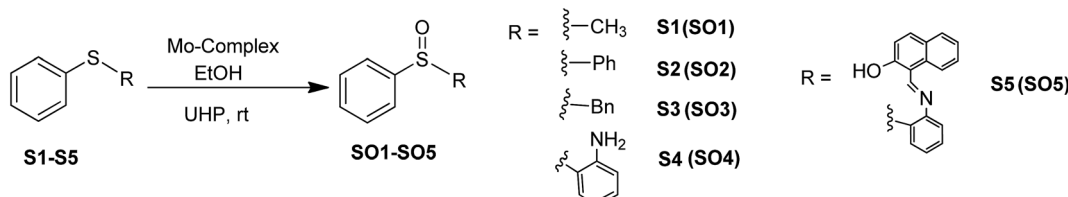
SHELX-97.²⁹ The crystallographic figures were generated using ORTEP 3v2 (ref. 30) and mercury 3.3.³¹

2.2. Preparation of complex 5

To a stirring solution of H₃L5 (0.1176 g, 0.30 mmol) in methanol (5 mL), MoO₂(acac)₂ (0.0978 g, 0.30 mmol) was added at room temperature and the reaction was continued for 13 h. The workup was done similarly to that reported for complex 2,¹⁸ to isolate the yellow solid product. Yield: 0.134 g (81%); mp: charred at 208–210 °C; UV-vis [λ_{max}; nm (ε; L cm⁻¹ mol⁻¹) in DMSO]: 260 (10 511), 348 (1980); IR (KBr; cm⁻¹): 3371, 1643, 1088, 903. ¹H NMR (DMSO-d₆, 400 MHz, ppm): δ 8.57 (1H, s, HC=N), 8.04 (1H, br, ArH), 7.61 (1H, d, *J* = 6.0 Hz, ArH), 6.89 (1H, d, *J* = 7.6 Hz, ArH), 5.65 (1H, br, glucose OH), 4.76 (2H, m, glucose H-1, ethylidene CH), 4.13 (4H, m, glucose H-5, methanolic-CH₃), 3.80–3.05 (5H, m, glucose, H-2, H-3, H-4, H-6a,b), 1.26 (3H, br, ethylidene CH₃); ¹³C NMR (DMSO-d₆, 100 MHz, ppm): δ 161.4 (C=N), 158.7, 137.7, 136.8, 123.1, 122.1, 110.7, 99.3, 91.2, 85.6, 81.0, 73.4, 69.9, 67.6, 49.0, 20.6; HRMS: *m/z* calcd for (M + H)⁺ C₁₅H₁₇BrMoNO₈ 515.9192; found 515.9358, without solvent.

2.3. Preparation of complex 6

This compound was prepared following the procedure adopted for complex 5, but using (H₃L6) (0.1020 g, 0.30 mmol) and MoO₂(acac)₂ (0.0978 g, 0.30 mmol). Yield: 0.130 g (89%); orange solid; mp: charred 233–235 °C; UV-vis [λ_{max}; nm (ε; L cm⁻¹ mol⁻¹) in DMSO]: 287 (12 336), 361 (2347); IR (KBr; cm⁻¹): 3333, 1643, 1088, 903. ¹H NMR (DMSO-d₆, 400 MHz, ppm): δ 8.52 (1H, s, HC=N), 7.32 (1H, d, *J* = 7.2 Hz, ArH), 7.19 (1H, d, *J* = 7.6, ArH), 6.91 (1H, m, ArH), 5.63 (1H, s, glucose OH), 4.72 (2H, m, ethylidene CH, glucose H-1), 4.18 (1H, m, glucose H-5), 3.90–3.10 (8H, m, glucose H-2, H-3, H-4, H-6a,b, methanolic-CH₃),



Scheme 1 Synthetic protocol of sulfoxides using sugar derived Mo(VI) complexes.

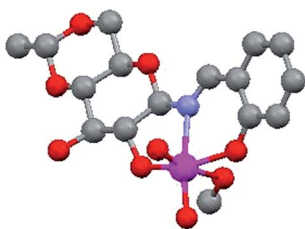


Fig. 2 Structure of 4,6-O-ethylidene-N-(2-hydroxybenzylidene)-D-glucopyranosylamine (H₃L1) derived *cis*-dioxo Mo(vi) complex.²⁷

Table 1 Summary of sulfide oxidation using D-glucose derived *cis*-dioxo molybdenum(vi) complexes as the catalyst^a and UHP as the mild oxidizing agent

Entry	Complex	Sulfoxide	Yield ^b (%)	TON	TOF/h
1	1	SO2	90	17.9	72
2		SO3	90	18.1	72
3		SO4	98	19.6	78
4		SO5	50	10	15
5	2	SO2	79	15.8	66
6		SO3	89	17.8	72
7		SO4	96	19.2	78
8		SO5	37 ^c	7.4	12
9	3	SO2	86	17.1	66
10		SO3	89	17.7	72
11		SO4	94	18.7	72
12		SO5	44 ^c	8.9	12
13	4	SO2	89	17.7	72
14		SO3	93	18.5	72
15		SO4	98	19.6	78
16		SO5	45 ^c	8.9	12
17	5	SO2	75	15	60
18		SO3	82	16.4	66
19		SO4	91	18.1	72
20		SO1	90	18	72
21		SO5	61 ^c	12.2	18
22	6	SO2	82	16.5	66
23		SO3	83	16.7	66
24		SO4	84	17	66
25		SO1	88	17.5	72
26		SO5	66 ^c	13.2	18

^a Refer to Fig. 1 for the structure of catalysts. ^b Yield (%) was calculated by HPLC after 15 min of reaction time. ^c Yield (%) was calculated by HPLC after 40 min of reaction time.

1.26 (3H, br, ethylidene CH₃); ¹³C NMR (DMSO-d₆, 100 MHz, ppm): δ 159.39 (C=N), 152.3, 149.5, 126.0, 121.3, 119.8, 117.2, 99.3, 91.1, 85.4, 81.1, 73.5, 69.9, 67.7, 56.2, 20.7; HRMS: *m/z* calcd for (M + H)⁺ C₁₆H₁₉MoNO₉ 467.0114; found 467.0102, without solvent.

2.4. Synthesis of [((2-(phenylthio)phenyl)imino)methyl]naphthalen-2-ol] (S5)

To the ethanolic solution of 2-hydroxynaphthaldehyde (1.01 mmol), **S4** (1 mmol) was added and the reaction mixture was refluxed for 8 h. The reaction mixture was cooled and the resultant yellow crystalline solid product was filtered, washed

with diethyl ether and dried under vacuum. Yield: 86%, yellow crystalline solid; mp: 140–142 °C; IR (KBr; cm⁻¹) UV-vis [λ_{max} ; nm (ϵ ; L cm⁻¹ mol⁻¹) in ethanol]: 315 (5599), 442 (4817), 465 (4531). ¹H NMR (CDCl₃, 400 MHz, ppm): δ 15.24 (1H, d, *J* = 2.4 Hz, ArOH), 9.40 (1H, d, *J* = 2.4 Hz, HC=N), 8.13 (1H, d, *J* = 8.4 Hz, ArH), 7.84 (1H, d, *J* = 9.2 Hz, ArH), 7.76 (1H, d, *J* = 7.6 Hz, ArH), 7.54 (1H, m, ArH), 7.48–7.14 (11H, m, ArH); ¹³C NMR (CDCl₃, 100 MHz, ppm) δ 167.6, 155.8, 145.7, 136.2, 134.0, 133.1, 132.2, 131.5, 131.1, 129.3, 129.3, 128.1, 128.0, 127.6, 127.5, 127.0, 123.6, 121.4, 119.1, 118.1, 109.3. Slow evaporation of the hexane solution of **S5** yielded X-ray suitable single crystals and the structure was established using single crystal X-ray crystallography.

2.5. General procedure for selective oxidation of organic sulfides

To a stirring suspension of molybdenum complexes (**1–6**; 0.05 mmol) and sulfides (1 mmol) in 3 mL of ethanol, UHP (1 mmol) was added at room temperature. The progress of the reaction was monitored by thin layer chromatography and upon completion of the reaction, yields were calculated by HPLC (Fig. S7–S9, ESI†).

2.6. Synthesis of [((2-(phenylsulfinyl)phenyl)imino)methyl]naphthalen-2-ol] (SO5)

This compound was prepared following the general procedure described above for sulfide oxidation, using **S5** (1 mmol), UHP (1 mmol) and complex **1** (0.05 mmol). After stirring the reaction mixture for 40 minutes at room temperature, pure **SO5** was separated from the reaction mixture using column chromatography on a silica gel solid support and ethyl acetate/hexane (30/70 v/v) as the eluent. Yield: 46%, yellow crystalline solid; mp: 142–143 °C; UV-vis [λ_{max} ; nm (ϵ ; L cm⁻¹ mol⁻¹) in ethanol]: 331 (5699), 386 (7598). ¹H NMR (CDCl₃, 400 MHz, ppm) δ 14.37 (1H, s, ArOH), 9.33 (1H, s, HC=N), 8.19 (1H, dd, *J* = 7.6, 1.7 Hz, ArH), 8.09 (1H, d, *J* = 8.4 Hz, ArH), 7.95 (1H, d, *J* = 9.2 Hz, ArH), 7.83 (1H, d, *J* = 8.0 Hz, ArH), 7.68 (2H, m, ArH), 7.63–7.54 (3H, m, ArH), 7.43 (1H, m, ArH), 7.35–7.25 (5H, m, ArH); ¹³C NMR (CDCl₃, 100 MHz, ppm) δ 163.6, 159.9, 145.8, 145.0, 139.1, 136.3, 132.7, 132.2, 131.1, 129.4, 129.2, 128.2, 127.9, 127.6, 125.7, 124.6, 123.9, 119.8, 119.3, 118.6, 109.4. Slow diffusion of hexane into a dichloromethane solution of **SO5** afforded X-ray suitable single crystals and finally the structure was confirmed by single crystal X-ray crystallography.

2.7. Catalyst recycling

Recycling of the catalyst was performed using complex **1** (0.05 mmol), **S4** (1 mmol) and UHP (1 mmol) in ethanol (3 mL) at room temperature. At the end of the first cycle of the reaction, the solvent was evaporated under reduced pressure and the pasty mass was extracted with dichloromethane (3 × 3 mL) to remove the sulfide and its oxidized products. The residue (complex **1**) was freshly treated with an equimolar amount of sulfide and UHP as mentioned above for the next cycle. The organic portion of the extract was used for isolation of the product using column chromatography.

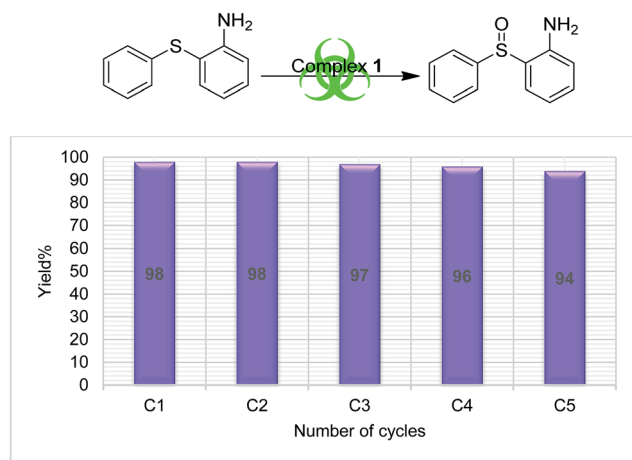


Fig. 3 Graphical representation of catalytic recyclability using complex 1 on S4.

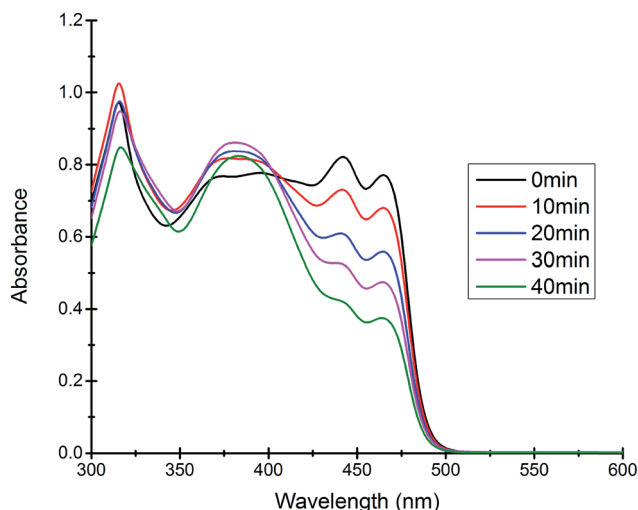


Fig. 4 Time dependent UV-visible spectra of the reaction mixture revealing the gradual decrease in the absorption band at 465 nm due to the consumption of the substrate S5.

2.8. Kinetic studies

A main reaction of complex **1** (0.005 mmol), sulfide **S5** (0.11 mmol), and UHP (0.11 mmol) in ethanol 10 (mL) was set at room temperature. 20 μ L of the reaction mixture was diluted to a final volume of 5 mL and its absorbance was measured at 465 nm using a UV-visible spectrophotometer. A decrease in the concentration of **S5** during the reaction at 298 K was monitored using a pre-generated calibration curve and the data was used to establish the order of the reaction.

3. Results and discussion

3.1. Synthesis and characterization of two new complexes

H_3L5 and H_3L6 were reacted with $MoO_2(acac)_2$ in methanol to yield the corresponding sugar containing molybdenum(vi) complexes. The formation of the complexes were confirmed by

FTIR, UV-visible, NMR and Mass spectroscopy. FTIR studies of both complexes exhibited strong characteristic vibration bands at 903, 1088, 1643 and 3333–3371 cm^{-1} corresponding to $\nu_{Mo=O}$, ν_{C-O} , $\nu_{C=N}$ and ν_{O-H} respectively. No appreciable changes were observed for ν_{C-O} and $\nu_{C=N}$ stretching frequencies of complexes with respect to their corresponding free ligands, but a substantial change was observed in the ν_{O-H} region of the spectra. Sharp bands in the OH region of the ligands converted into a broad one after the metalation reaction, indicating the increment in hydrogen bonding interactions. The peak at 13.01 and 5.33 ppm corresponding to the phenolic and C2-hydroxyl proton of glucose respectively in the ligand, disappeared from the 1H NMR spectra of the molybdenum complexes revealing the metal complexation *via* the phenolate and alcalate group. In both complexes, the signal of glucose C3-OH shifted down field with respect to the free ligands, which might be attributed to the change in electronic environment contributed by the chelated metal ion. All these spectral changes are consistent with the spectral description of reported similar Mo(vi) complexes of H_3Ln ($n = 1-4$).^{18,27}

3.2. Selective oxidation of sulfide to sulfoxide

The molecular structure of 4,6-O-ethylidene-*N*-(2-hydroxybenzylidene)- β -D-glucopyranosylamine (H_3L1) derived Mo(vi) complex (Fig. 2) has already been established²⁷ and a similar complex has also been reported by Zhao *et al.*,³² using a glucosamine derived ligand. The literature is rich with the catalytic reactions of di-oxo Mo(vi) complexes,^{33–35} however it is scarce for sugar derived from such molecules. Zhao *et al.* published catalytic epoxidation reactions,³² we have reported the selective synthesis of a series of bis(indolyl)methanes by condensing indole derivatives with carbonyl compounds,³⁶ while Mohammadnezhad *et al.*³⁷ and our group have recently communicated the oxidation of **S1** to **SO1**.¹⁸ We had reported the optimization of reaction conditions with respect to catalytic loading, solvent effect, reaction time *etc.* on a single substrate **S1**. In continuation of our previous work, we have tried to develop a general protocol for sulfide oxidation by sugar derived *cis*-dioxo Mo(vi) complexes and, in the process, the number of catalysts as well as substrates have been increased. All the reactions were performed under optimized conditions developed by us for sulfoxide formation,¹⁸ *i.e.*, ethanol as the reaction solvent and a shorter reaction time (15 min) using a 1 : 1 molar ratio of sulfides and UHP. In order to better understand the conversion and purity, we have calculated the yields of product formation using HPLC and details of the method is stated in the experimental section. We have achieved the conversion with good to excellent yields and the same is summarized in Table 1. The formation of **SO1**–**SO4** was established by comparing the respective melting points, IR, NMR and ESI-MS (characterization data and Fig. S10–S18: ESI†) spectra with the reported literature.^{17,18,38,39} Sheikhshoaei *et al.* have also done similar reactions using a 2-[(2-hydroxypropylimino)methyl]phenol derived Mo(vi) complex as the catalyst and UHP as a mild oxidant⁴⁰ and our results are comparable to them. Varma and Naicker have reported the oxidation of **S1** using UHP without

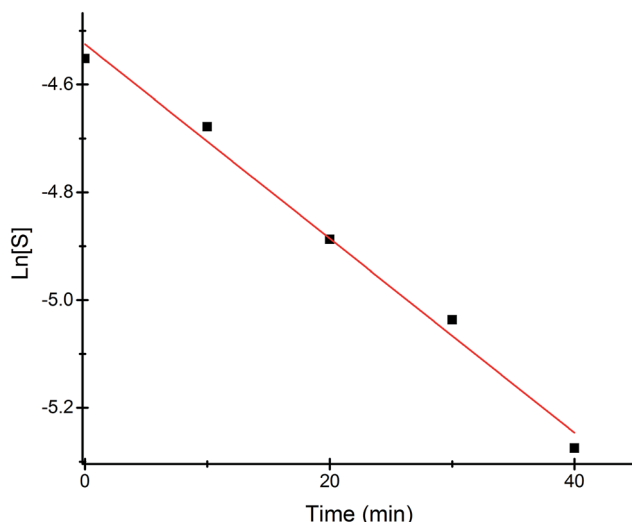


Fig. 5 Linear fitting plot of $\ln[S5]$ vs. time at 298 K.

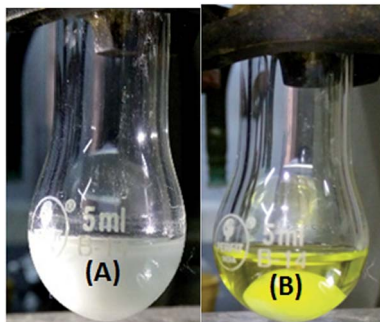
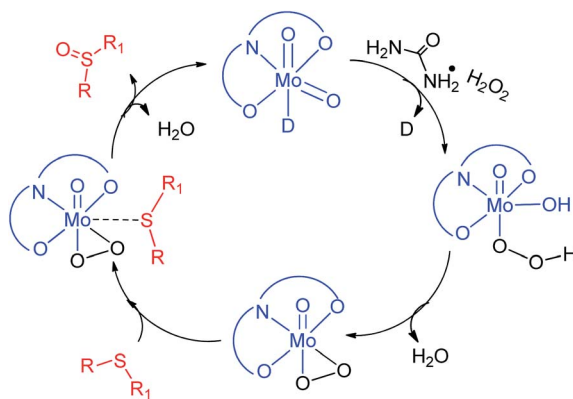


Fig. 6 (A) Complex 1 in ethanol and (B) complex 1 in ethanol after UHP addition.



Scheme 2 Proposed mechanistic pathway for the formation of sulfoxide.

any catalyst but at 85 °C and the yield was 80%.⁴¹ So, the use of a catalyst has not only reduced the reaction temperature but also improved the yield and purity of the product as they noticed a 10% mixture of sulfone.

In order to understand the stability of catalysts during the catalytic reaction, a recyclability test was performed using complex **1** and **S4** as a substrate. The catalyst was recycled five times (methods explained in Experimental section), and the results are presented in Fig. 3, which clearly supports the reliability of the catalytic process. No appreciable change in the catalytic efficiency was observed as the sulfoxide formation was in the range of 98 to 94%, from the first cycle to the end of the fifth cycle respectively.

The literature supports that it is easy to oxidize organic sulfides having electron-donating substituents than one having electron withdrawing groups.⁴² Our finding also followed this trend as we found the lowest yields (37–66%) for the oxidation of **S5**, while the highest (84–98%) were found for compound **S4**. The salient feature of the present sulfoxidation protocol is its high selectivity to form only sulfoxide and neither sulfones nor an oxidized benzylic product with substrate **S3**.

3.3. Kinetic studies

Most of the commercially available general organic sulfides and their corresponding sulfoxides exhibit a common overlapping absorption band in the UV-visible spectra. In our case, the spectral pattern of **S1–S4** behaved similarly and the rate of oxidation was also fast. So, in order to understand the overall order of the reaction, we planned to develop a sulfide which should have a slow rate of oxidation along with a non-overlapping absorption band in the UV-visible spectrum for the substrate and corresponding oxidized product. In this venture, we synthesized a new sulfide **S5**, which fulfilled both criteria and hence the kinetics of the reaction was explored on this molecule using UV-visible spectroscopy. A comparison of UV-visible absorption spectra of the reactants (Fig. S-23, ESI†) revealed that only **S5** absorbs at 465 nm and hence the oxidation reaction was monitored by measuring the absorbance of this band with course of time at 298 K. A decrease in absorbance at 465 nm was measured for the first 40 min (Fig. 4) and the data was analyzed. A linear $\ln[S5]$ vs. time plot (Fig. 5) supported the overall first order reaction kinetics with a rate constant, $k = 0.01804 \text{ min}^{-1}$ and a half-life, $t_{1/2} = 38.4$ minutes.

3.4. Mechanism of reaction

In order to gain insight into the reaction mechanism, sulfide **S2** was added to the ethanolic solution of the molybdenum complex **1** while stirring. No visual change in the physical appearance of the reaction mixture was noticed even after 15 min of stirring. The reaction mixture was analyzed using a UV-visible spectrophotometer (Fig. S-24, ESI†), however no interaction between complex **1** and sulfide **S2** was established. Similar studies performed using an ethanolic solution of sulfide **S2** and UHP (Fig. S-25, ESI†) also failed to establish the interactions. Finally, molybdenum complex **1** was suspended in ethanol and UHP was added to that, which resulted in an instantaneous yellowish transparent solution (Fig. 6). The UV-visible absorption studies (Fig. S-26, ESI†) on these sets of control reactions also supported the interaction *via* the

Table 2 Summary of the crystallographic data and structural parameters of **S5** and **SO5**

	S5	SO5
Empirical formula	$C_{23}H_{17}NOS$	$C_{23}H_{17}NO_2S$
Molecular weight	355.43	371.43
<i>T</i> (K)	100	100
Crystal system	Orthorhombic	Orthorhombic
Space group	$P2_12_12_1$	$P2_12_12_1$
Cell constants		
<i>a</i> (Å)	6.132(2)	5.6260(10)
<i>b</i> (Å)	14.536(5)	12.886(2)
<i>c</i> (Å)	19.327(7)	24.399(5)
<i>V</i> (Å ³)	1722.6(11)	1768.8(6)
<i>Z</i> value	4	4
<i>D</i> _{calcd} (g cm ⁻³)	1.371	1.395
Total reflections	11 726	15 463
Unique reflections	3922	4029
Parameters	236	245
Final <i>R</i> (<i>I</i> > 2σ(<i>I</i>))	0.0910	0.0627
<i>R</i> _w	0.2135	0.1231

hypochromic effect along with an overall change in the peak positions.

Furthermore, the effect of the variation in UHP concentration was studied, where no change in the kinetics of the reaction was noticed, however an increase in the conversion of sulfides into sulfones was observed. All these studies concluded that the binding of UHP with the molybdenum complex occurs at the initial stage of the sulfide oxidation reaction. A similar finding has also been reported by Kamata *et al.*,⁴³ Panda *et al.*⁴⁴ and Chakravarthy *et al.*⁴⁵ using W, Ti and Mo complexes respectively, however all of them have used H_2O_2 as an oxidizing agent. Chakravarthy *et al.* have proposed the possibility of sulfide binding with either a molybdenum center or peroxy oxygen.⁴⁵ The literature reveals that an increase in electron density about sulfur due to its attachment with electron donor groups increases the oxidation efficiency and we also noticed the same trend. This fact is only possible if sulfide is interacting with a metal center and not with peroxy oxygen, as the electronegative nature of oxygen will repel the electron rich sulfur centre. Hence, in our opinion, sulfide ion binds with the Mo center rather than peroxy oxygen. On the basis of our results and the previous literature reports^{43–45} a plausible oxidation mechanism has been summarized in Scheme 2.

3.5. Crystal structure of **S5** and **SO5** and their correlation with the oxidation process

Among all the sulfides used in this paper, the rate of oxidation as well as yields were the lowest for **S5**. The low yield is attributed to the formation of sulfoxide at the initial stage followed by parallel formation of sulfide and sulfones, while the low rate of oxidation might be due to either steric crowding or the electronic environment or both together about the sulfur center. In order to understand this chemistry, we crystallized both the sulfide (**S5**) and corresponding sulfoxide (**SO5**) and their solid state structure was established using single crystal X-ray crystallography. In both cases, crystal quality was averaged and the *R* values (0.0910 and 0.0627) were within the accepted range for publication as mentioned in the crystallographic summary (Table 2). The ORTEP plot of **S5** shown in Fig. 7(a) indicates the hindrance of the sulfide ion to come closer to the Mo center of the catalyst and the same can be clearly viewed in the space-filling model (Fig. 7(b)). The whole molecule is arranged in space such that three sides of the basal plane of sulfur is covered with naphthyl and phenyl rings, while the perpendicular arrangement of one of the phenyl rings obstructs its exposure to the catalyst from the vertical side. Such an atomic environment about sulfur might be responsible for its slow oxidation process as it might not be able to interact with the catalytic center appropriately.

Since the environment about sulfur is crowded in **S5**, it raises a curiosity to know about the special arrangement of molecular fragments in **SO5**. In order to fulfill this inquisitiveness, the solid state structure of **SO5** was explored using single crystal X-ray crystallography. The ORTEP plot of **SO5** with an atomic labeling scheme is presented in Fig. 8(a), while Fig. 8(b) illustrates its space-filling model. This structure clearly reveals the overall change in the atomic environment about sulfur, which facilitates it to protrude out, which might help it in converting to sulfone parallel to sulfide oxidation. The changes in conformations of sulfide and sulfoxide can be easily established by analyzing the selected torsion angles. The angles C(1)N(1)C(12)C(17), C(10)C(2)C(1)N(1), C(14)C(13)S(1)C(18) and C(13)S(1)C(18)C(19) are 15.9(11), 179.4(7), 9.5(8) and –113.5(7) in sulfide, while –36.0(7), 170.6(4), –106.0(4) and 6.6(5) respectively in sulfoxide.

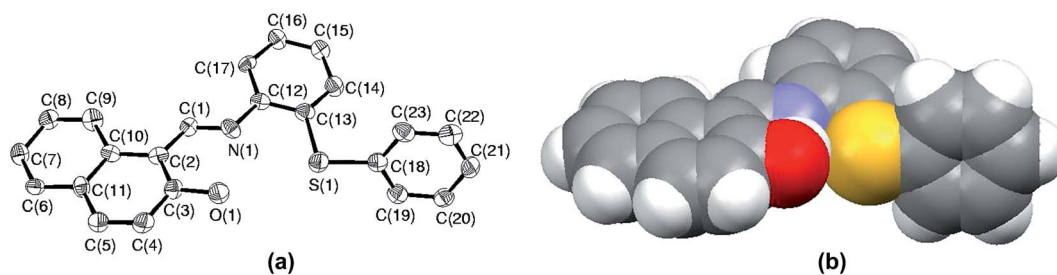


Fig. 7 (a) ORTEP plot of **S5** drawn using 50% probability ellipsoids; (b) space-filling model of **S5** showing the hindrance about the sulfur atom.

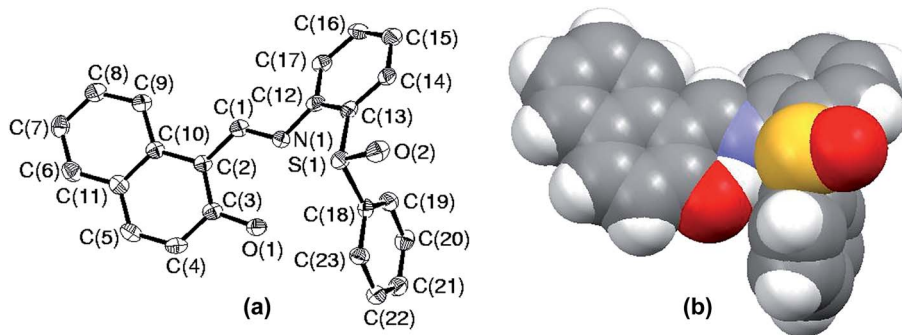


Fig. 8 (a) ORTEP plot of SO5 drawn using 50% probability ellipsoids; (b) space-filling model of compound SO5.

4. Conclusions

Selective oxidation of organic sulfides to sulfoxides have been explored using glucose derived *cis*-dioxo molybdenum(vi) complexes as catalysts and urea–hydrogen peroxide as a mild oxidising agent. A total of six catalysts were tested on five sulfides and good to excellent conversion was achieved under milder reaction conditions and shorter reaction time. The conversion was best for compound S4 (84–98%) and least for compound S5 (37–66%). All the yields were calculated using HPLC separation and the purity of the products was further checked by comparing their melting point, FTIR and NMR data with the literature values. A new sulfide S5 and corresponding sulfoxide SO5 also has been developed and their structures have been established using the single crystal X-ray diffraction method. One of the catalysts was tested for recyclability and only a minute change (~4% loss) in activity was observed during five cycles, revealing the sustainability of the catalyst under the reaction conditions. Even though similar reactions are reported using other catalysts and conditions, the advantage of our report is the greener methodology *i.e.*, catalyst consisting of bio-viable species (D-glucose and molybdenum), short reaction time, high selectivity, room temperature reaction and ethanol as the reaction medium. This paper also deals with the kinetics and mechanistic aspects of sulfide oxidation.

Acknowledgements

We are thankful to Dr Angshuman Roy Choudhury for his help in crystallographic data collection. A. K. Sah is grateful to Department of Science and Technology (DST) and University Grants Commission (UGC) for the financial support. The Department of Chemical Sciences, Indian Institute of Science Education and Research, Mohali is acknowledged for providing the XtaLABmini X-ray diffractometer facility. We are also thankful to DST FIST and UGC SAP for their financial support in procuring the instruments and developing the research infrastructure.

References

- 1 M. C. Carreño, *Chem. Rev.*, 1995, **95**, 1717–1760.
- 2 I. Fernández and N. Khiar, *Chem. Rev.*, 2003, **103**, 3651–3705.
- 3 A. M. Khenkin and R. Neumann, *J. Am. Chem. Soc.*, 2002, **124**, 4198–4199.
- 4 S. J. Danishefsky and B. Simoneau, *J. Am. Chem. Soc.*, 1989, **111**, 2599–2604.
- 5 A. B. Jones, M. Yamaguchi, A. Patten, S. J. Danishefsky, J. A. Ragan, D. B. Smith and S. L. Schreiber, *J. Org. Chem.*, 1989, **54**, 17–20.
- 6 G. H. Posner, J. P. Mallamo and K. Miura, *J. Am. Chem. Soc.*, 1981, **103**, 2886–2888.
- 7 D. H. Hua, S. Venkataraman, R. Y. K. Chan and J. V. Paukstelis, *J. Am. Chem. Soc.*, 1988, **110**, 4741–4748.
- 8 G. Solladié, in *Asymmetric Synthesis*, ed. J. D. Morrison, Academic Press, New York, 1983.
- 9 D. H. Hua, in *Advances in Carbanion Chemistry*, ed. V. Snieckus, JAI Press, London, 1992.
- 10 D. H. Hua, *Adv. Heterocycl. Nat. Prod. Synth.*, 1996, **3**, 151.
- 11 Y. Arai and T. Koizumi, *Sulfur Rep.*, 1993, **15**, 41–65.
- 12 P. Renaud, *Chimia*, 1997, **51**, 236–238.
- 13 P. Renaud and M. Gerster, *Angew. Chem., Int. Ed.*, 1998, **37**, 2562–2579.
- 14 J. Legros and C. Bolm, *Angew. Chem., Int. Ed. Engl.*, 2004, **43**, 4225–4228.
- 15 D. A. Cogan, G. Liu, K. Kim, B. J. Backes and J. A. Ellman, *J. Am. Chem. Soc.*, 1998, **120**, 8011–8019.
- 16 H. Egami and T. Katsuki, *Synlett*, 2008, **10**, 1543–1546.
- 17 Z. Wang, A. Q. Peng, X. L. Sun and Y. Tang, *Sci. China: Chem.*, 2014, **57**, 1144–1149.
- 18 A. K. Sah and N. Baig, *Catal. Lett.*, 2015, **145**, 905–909.
- 19 J. Fridgen, W. A. Herrmann, G. Eickerling, A. M. Santos and F. E. Kühn, *J. Organomet. Chem.*, 2004, **689**, 2752–2761.
- 20 T. Fujihara, Y. Sasaki and T. Imamura, *Chem. Lett.*, 1999, **5**, 403–404.
- 21 W. S. Liu, R. Zhang, J. S. Huang, C. M. Che and S. M. Peng, *J. Organomet. Chem.*, 2001, **634**, 34–38.
- 22 J. T. Spence and J. Tocatlian, *J. Am. Chem. Soc.*, 1961, **83**, 816–819.
- 23 R. Cammack, M. J. Barber and R. C. Bray, *Biochem. J.*, 1976, **157**, 469–478.
- 24 G. Vujevic and C. Janiak, *Z. Anorg. Allg. Chem.*, 2003, **629**, 2585–2590.
- 25 R. Hille, *Chem. Rev.*, 1996, **96**, 2757–2816.

26 R. H. Holm, P. Kennepohl and E. I. Solomon, *Chem. Rev.*, 1996, **96**, 2239–2314.

27 A. K. Sah, C. P. Rao, P. K. Saarenketo, E. K. Wegelius, E. Kolehmainen and K. Rissanen, *Eur. J. Inorg. Chem.*, 2001, **2001**, 2773–2781.

28 Rigaku Corporation 2000–2010, Tokyo 196-8666, Japan.

29 G. M. Sheldrick, *Acta Crystallogr., Sect. A: Found. Crystallogr.*, 2008, **64**, 112–122.

30 L. J. Farrugia, *J. Appl. Crystallogr.*, 1997, **30**, 565.

31 A. L. Spek, *Acta Crystallogr., Sect. D: Biol. Crystallogr.*, 2009, **65**, 148–155.

32 J. Zhao, X. Zhou, A. M. Santos, E. Herdtweck, C. C. Romão and F. E. Kühn, *Dalton Trans.*, 2003, 3736–3742.

33 R. D. Chakravarthy and D. K. Chand, *J. Chem. Sci.*, 2011, **123**, 187–199.

34 K. Jeyakumar and D. K. Chand, *J. Chem. Sci.*, 2009, **121**, 111–123.

35 J. A. Schachner, P. Traar, C. Sala, M. Melcher, B. N. Harum, A. F. Sax, M. Volpe, F. Belaj and N. C. Mösch-Zanetti, *Inorg. Chem.*, 2012, **51**, 7642–7649.

36 N. Baig, G. M. Shelke, A. Kumar and A. K. Sah, *Catal. Lett.*, 2016, **146**, 333–337.

37 G. Mohammadnezhad, R. Debel and W. Plass, *J. Mol. Catal. A: Chem.*, 2015, **410**, 160–167.

38 R. L. Shriner, H. C. Struck and W. J. Jorison, *J. Am. Chem. Soc.*, 1930, **52**, 2060–2069.

39 B. Zhang, M. D. Zhou, M. Cokoja, J. Mink, S. L. Zang and F. E. Kühn, *RSC Adv.*, 2012, **2**, 8416–8420.

40 I. Sheikhshoaei, A. Rezaeifard, N. Monadi and S. Kaafi, *Polyhedron*, 2009, **28**, 733–738.

41 R. S. Varma and K. P. Naicker, *Org. Lett.*, 1999, **1**, 189–191.

42 C. J. Carrasco, F. Montilla, E. Álvarez, C. Mealli, G. Manca and A. Galindo, *Dalton Trans.*, 2014, **43**, 13711–13730.

43 K. Kamata, T. Hirano, R. Ishimoto and N. Mizuno, *Dalton Trans.*, 2010, **39**, 5509–5518.

44 M. K. Panda, M. M. Shaikh and P. Ghosh, *Dalton Trans.*, 2010, **39**, 2428–2440.

45 R. D. Chakravarthy, K. Suresh, V. Ramkumar and D. K. Chand, *Inorg. Chim. Acta*, 2011, **376**, 57–63.